

STRUCTURAL PERFORMANCE OF A HYBRID TIMBER WALL SYSTEM FOR EMERGENCY HOUSING FACILITIES

Daniele Casagrande¹, Ester Sinito¹, Matteo Izzi¹, Gaia Pasetto¹, Andrea Polastri^{1*}

Abstract

This paper presents an innovative and sustainable timber constructive system that could be used as an alternative to traditional emergency housing facilities. The system proposed in this study is composed of prefabricated modular elements that are characterized by limited weight and simple assembly procedures, which represent strategic advantages when it comes facing a strong environmental disaster (e.g. an earthquake). The complete dismantling of structural elements and foundations is granted thanks to specific details and an innovative connection system called X-Mini, capable of replacing traditional anchoring devices (i.e. hold downs and angle brackets) by resisting both shear and tension loads. This constructive system, denoted as Hybrid Timber Frame (HTF), takes advantage of the strong prefabrication, reduced weight of light-frame timber systems, and of the excellent strength properties of the Cross Laminated Timber (CLT) panels. Specifically, the solid-timber members typically used in the structural elements of light-frame systems are replaced by CLT linear elements. The results of experimental tests and numerical simulations are critically presented and discussed, giving a detailed insight into the performance of the HTF under seismic conditions.

¹National Research Council of Italy – Institute of Bioeconomy (CNR-IBE), Via Biasi 75, 38010 San Michele all'Adige, Italy.

* Corresponding author.

Email addresses: daniele.casagrande@ibe.cnr.it (D. Casagrande), andrea.polastri@ibe.cnr.it (A. Polastri).

19 **Keywords**

20 Emergency structure, innovative connection, temporary building, hybrid timber frame, seismic
21 behaviour.

22 **1. Introduction**

23 *1.1 Objectives of research*

24 The importance of emergency housing facilities in Italy has been recently highlighted because
25 of the occurrence of strong earthquakes and the migrant flows into Europe. In this context,
26 providing shelter to the displaced people and the refugees has become a critical issue in the
27 management of the post-emergency phases. Despite the lack of specific Standards, several
28 strategies have been pursued in accordance with the National Guidelines that were released
29 in 2005 by the Italian Civil Protection Department (ICPD) [1, 2]. Those guidelines specify that
30 tent cities are usually erected immediately after the disaster to supply the primary needs of
31 the population. Temporary housing units (denoted with the acronym of MAP, which stands for
32 “*Modulo Abitativo Provvisorio*” in Italian) are assembled afterwards, to be used by the
33 population during the reconstruction of the damaged buildings. Nevertheless, the use of
34 temporary units has pointed out several limitations, which are related to the economic costs,
35 the complexity of the management operations, the duration of assembling and dismantling
36 phases, as well as several sustainability issues.

37 To overcome the limitations reported above, a team of the National Research Council of Italy
38 - Institute of Bioeconomy (CNR-IBE), former CNR-IVALSA, focused on developing a new
39 timber construction system in the following denoted as “Hybrid Timber Frame” (HTF). The
40 research works that lead to the definition of the HTF wall system were carried out within the
41 framework of the TRE3 research project [34]. The technology used in the Light Frame Timber
42 (LFT) constructions was used as the basis for the study. However, to enhance the

43 sustainability of such a system, the solid-timber elements used for the structural members of
44 LFT systems have been replaced with CLT elements that were obtained as secondary
45 products from the cutting process of CLT master-panels (i.e. from the openings of doors and
46 windows). Furthermore, an innovative connection system was specifically developed to speed
47 up the assembling and dismantling phases. The HTF structural system analysed in the paper
48 can be considered an evolution of the traditional LFT systems and it is a viable alternative to
49 traditional constructive systems also in the case of permanent structures. Experimental tests
50 and numerical analyses were carried out to assess the performance of the structural elements
51 (both connections and shear-wall modules) with specific attention to their performance in case
52 of a seismic event.

53 *1.2 Emergency housing facilities in Italy*

54 The need of emergency housing facilities arises after a catastrophic event (an environmental
55 disaster, a conflict, or the migrant flows) and is associated to a quantitative and/or a qualitative
56 lack of habitations due to destroyed or damaged buildings. In such a situation, it is necessary
57 to provide the displaced people with a shelter and a secure settlement, assuring reasonable
58 living conditions for a certain period of time. The strong earthquakes occurred in Italy over the
59 last twenty years (i.e. Molise in 2002, L'Aquila in 2009, Emilia in 2012, Amatrice in 2016) have
60 brought under the light several issues related to the management of post-emergency phases
61 and have emphasized the key-role of temporary housing facilities.

62 As reported in the introduction, tent cities represent the space where people gather for a short
63 period of time immediately after a disaster. Prefabricated structures, such as containers and
64 trailers, are generally used afterwards to accommodate the population before the installation
65 of the transitional (i.e. MAP) housing units (e.g. Irpinia Earthquake in 1980, Umbria
66 Earthquake in 1997, and Molise Earthquake in 2002). MAP units play a key role in all
67 subsequent phases, because are used by the population while the reconstruction occurs.

68 Nevertheless, it is important to notice that a different strategy was pursued in 2009 after
 69 L'Aquila Earthquake, when the permanence in the tents was protracted up to the complete
 70 erection of MAP units [3], see Figure 1.

71 Despite their extensive use, the construction and management process of MAP units pointed
 72 out two relevant issues and limitations of transitional houses. Specifically, because MAP units
 73 are erected using traditional constructive processes, the displaced people are forced to stay
 74 in the tents for a long period of time, causing some health and social problems, especially if
 75 containers are not used as intermediate solutions. Furthermore, MAP units are designed to
 76 accommodate the population for a short-to-medium period of time (2-to-24 months after the
 77 earthquake). However, those structures have been erected by considering some constructive
 78 details typical of permanent buildings, without a specific attention to the dismantling process.

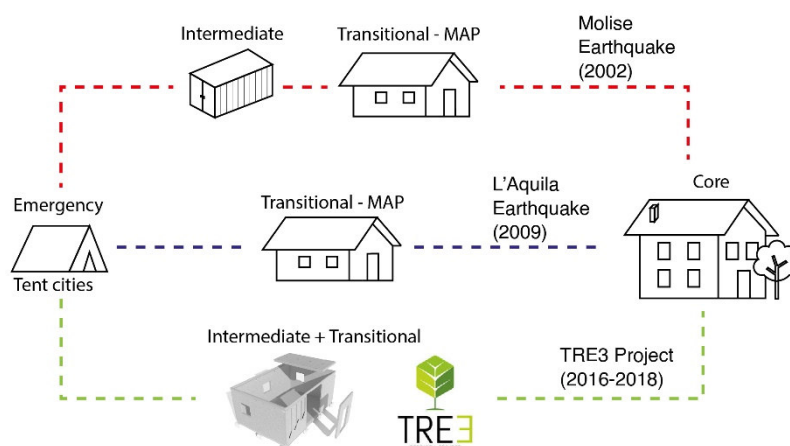


Figure 1: Temporary models for emergency housing facilities.

81 Materials, building process, maintenance, dismantling and reuse [3, 4] are crucial aspects
 82 when developing a sustainable model for temporary or transitional housing facilities.
 83 Specifically, the sustainability of constructions is an important challenge to limit the
 84 environmental impact in terms of greenhouses gases emission and land-use. To this aim, a
 85 sustainable approach to the planning of temporary facilities should consider the complete
 86 dismantling and the re-use (total or at least partial) of shelter units and of their foundations,
 87 with benefits on the use of natural resources and land.

2.1 Seismic behaviour of traditional LFT and CLT structural systems

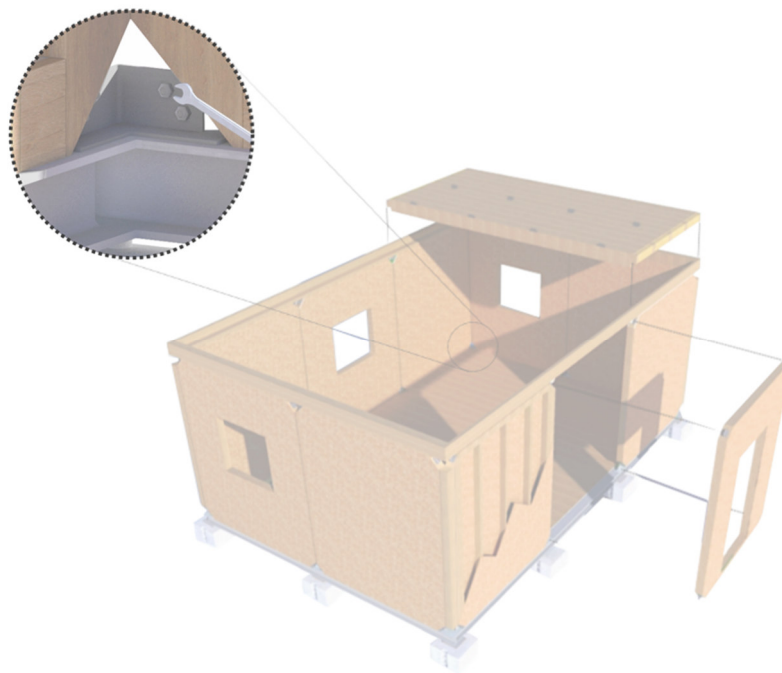
90 In recent years, the mechanical performance of LFT and CLT structures has been the focus
91 of a large body of research. Extensive experimental campaigns addressed the behaviour of
92 typical LFT and CLT lateral load-resisting systems with specific attention to their applications
93 in multi-storey structures. Results of LFT systems showed that their high seismic performance
94 is associated to the limited weight of shear walls and the localization of most of the plastic
95 deformations in the sheathing-to-framing connections. In this context, Filiatrault et al. [6]
96 carried out full-scale shaking table tests on a two-storey LFT building determining the dynamic
97 properties under different input intensities, whereas Van de Lindt et al. [7] performed similar
98 tests on a six-storey LFT building within the Neeswood project. Seim et al. [8] performed a
99 comparative study on the cyclic behavior of sheathing-to-framing joints with nailed Oriented
100 Strain Board (OSB) and stapled Gypsum Fibre Boards (GFB) panels. Tomasi et al. [9]
101 performed shaking table tests on a prefabricated three-storey timber-frame building in which
102 no damages were detected up to a peak ground acceleration of 1.0 *g*. Finally, Casagrande et
103 al. [10] presented the results of full-scale shaking table tests carried out within the European
104 SERIES Project on a three storey light-frame timber building with GFB panels.

105 Conversely, the CLT structures proved to be a valid solution for low-rise and mid-rise buildings
106 erected in seismic areas thanks to the significant in-plane stiffness and strength of CLT panels
107 and the good dissipative behaviour achieved in the anchoring systems [11]. The outcomes of
108 a comprehensive research project called 'SOFIE' were presented by Ceccotti et al. [12] and
109 proved the suitability of multi-storey CLT structures for earthquake-prone regions. Within the
110 European SERIES Project, Flatscher and Schickhofer [13] presented the results of bi-axial
111 shaking table tests of a three-storey CLT structure, highlighting the limited lateral deformability
112 of the building. Popovski and Gavric [14] carried out quasi-static load tests on a two-storey

113 building, while Kawai et al. [15] analysed the dynamic behaviour of a five-storey and a three-
114 storey CLT buildings. Finally, Yasumura et al. [16] investigated the performance of two two-
115 storey CLT buildings by comparing their seismic behavior when erected using either large
116 monolithic walls or narrow CLT panels, respectively.

117 2.2 The TRE3 research project

118 The TRE3 research project introduces an innovative timber constructive system that could be
119 used to erect one-storey emergency housing facilities [34]. This system consists of a new
120 type of timber-frame wall module, i.e. HTF, which represents an alternative to: a) modular
121 prefabricated housing units (such as containers), which are usually assembled in factory and
122 require heavy transport and lifting systems [5]; b) MAP units, often used as permanent houses
123 rather than as temporary constructions without paying attention to their environmental impact.

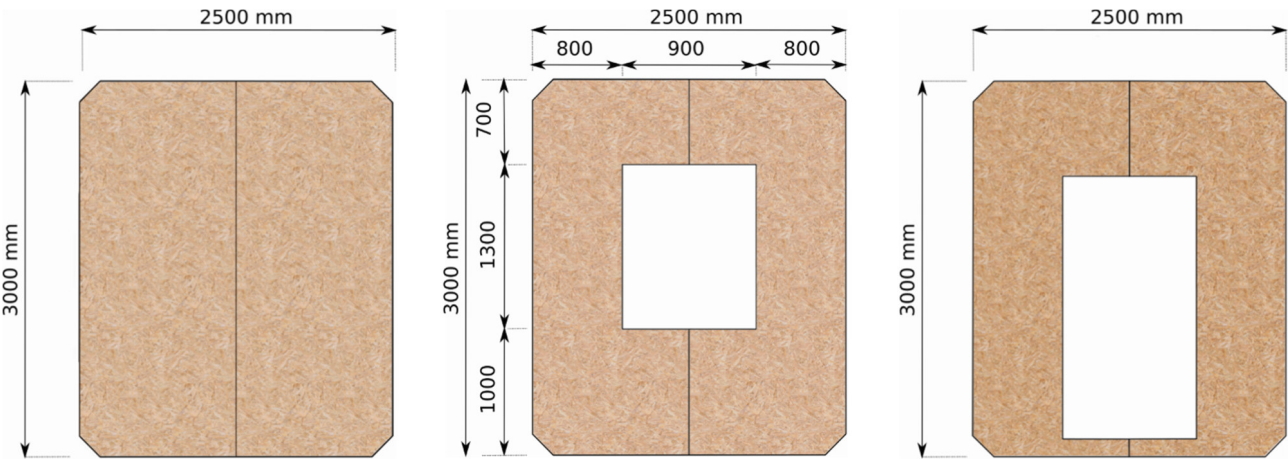


124

125 **Figure 2: Emergency housing facility built with the HTF wall modules.**

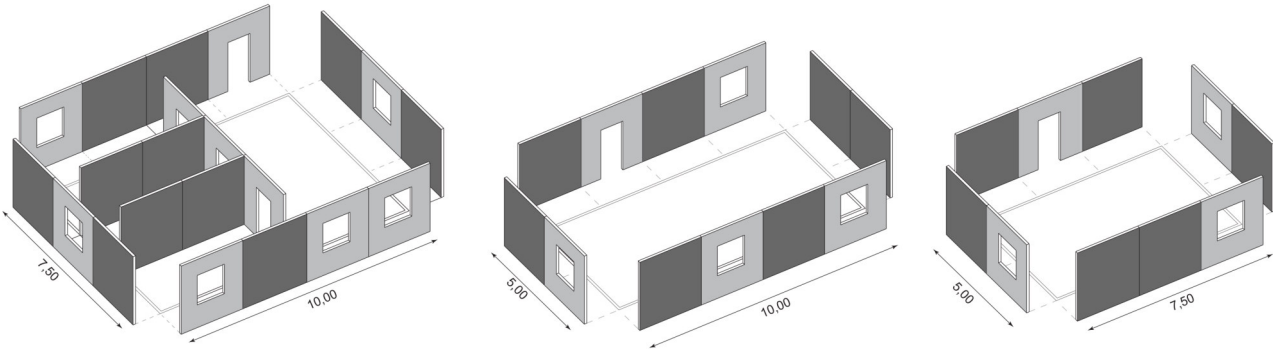
126 The HTF wall system is based on prefabricated 2D modules with dimensions of 2.5 m by 3.0
127 m, see Figure 2. The 2D wall elements can be transported using non-exceptional carriages,
128 simplifying the access to construction sites especially in places that have been impacted by

129 an earthquake. Furthermore, unlike a CLT wall system, the limited weight of the HTF module
 130 represents an advantage during the assembling phases. To ensure the modularity of the HTF
 131 system, three basic modules have been identified as shown in Figure 3): a wall-module, a
 132 door-module and a window-module.



133 **Figure 3: Schematic representation of the three HTF modules: wall-module, window-module and door-**
 134 **module. Dimensions expressed in (mm).**

135 Depending on the number of inhabitants expected, the three HTF basic modules allow
 136 assembling different types of emergency housing facilities, characterised by various spatial
 137 configurations. To this aim, three configurations have been analysed within the framework of
 138 the TRE3 research project, characterised by a footprint of 36 m², 49 m² and 73.5 m²,
 139 respectively (Figure 4).



140
 141 **Figure 4: Schematic representation of the three case studies (dimensions in m).**

142 Each HTF module is equipped with an innovative connection system, purposely developed

143 within the TRE3 research project and labelled *X-Mini*. Differently from a traditional LFT wall,
144 all mechanical anchors (hold-downs and angle brackets) are replaced with this preassembled
145 connection system installed at the four corners of the panel. During the assembling phases,
146 the X-Mini simply requires to be bolted to the foundations without additional screws or nails.
147 Each wall module can hence be dismantled and re-used in a different location by means of
148 few and fast on-site operations. Furthermore, traditional permanent foundations (usually
149 concrete platforms) are replaced with a prefabricated system composed of a grid of steel
150 beams and punctual concrete support elements.

151 **3. Mechanical behavior of the HTF wall module**

152 *3.1 The HFT wall system*

153 The HTF wall system is an evolution of the LFT wall, where the outer timber members of the
154 structural frame (i.e. top and bottom beams, and outer studs) are made with CLT elements.
155 Traditional wood-panels (e.g. OSB) are adopted as sheathing elements on one or both sides
156 of the wooden frame, while the inner studs are made of traditional solid timber, see Figure 5.

157 The advantages of adopting CLT members rather than solid wood members in a LFT wall are
158 noteworthy. In particular, the adoption of CLT members on the outer elements allows using
159 preassembled connection systems (e.g. the X-RAD system [17]) that work in the same plane
160 of the wall. This permits to avoid all brittle failure mechanisms related to either an eccentricity
161 between the wall and the connections or due to the sheathing panel interlayered between the
162 anchoring devices and the outer studs. Moreover, the use of such a type of connector ensures
163 a fast and easy building process, as well as a complete dismantling of the structural walls.

164 *3.2 The X-Mini connection system*

165 Each HTF module is equipped with an innovative connection system called X-Mini, Figure 6,

166 capable of resisting simultaneously both the shear and tension loads, and of replacing the
167 traditional anchoring devices (i.e. hold downs and angle brackets). This connection system is
168 pre-installed at the four corners of the panel and, during the assembling phases, it simply
169 requires to be bolted to the foundations without additional screws or nails. Thanks to this
170 anchoring system, each wall module can be dismantled and re-used in a different location by
171 means of few on-site operations. Furthermore, the traditional permanent foundations (typically
172 concrete platforms) are replaced with a prefabricated system composed of a grid of steel
173 beams and punctual concrete support elements.

174 Four X-Mini are secured at the top and bottom corners of the CLT outer studs by means of 9
175 x 240 mm fully threaded screws, see Figure 5. Each X-Mini is made of cold-formed steel
176 plates with thickness of 4 mm and has a total size of 100 mm (length) by 70 mm (height) by
177 70 mm (width). The two vertical screws are fastened to the outer stud to bear the tensile
178 component of the load and two horizontal screws are anchored to the bottom beam to transfer
179 the horizontal load to the foundations. Because the two horizontal screws pass through both
180 the outer stud and the bottom beam, the anchoring between the two CLT elements is ensured.
181 The symmetry axis of the X-Mini is inclined at 45° with respect to the outer stud.

182 X-Mini was conceived starting from X-RAD [18] which was explicitly designed to be used in
183 multi-storey CLT buildings and is able to transmit a large amount of load (between 100 kN
184 and 200 kN, depending on the direction of the acting load). X-RAD consists of a point-to-point
185 connection system, screwed to the corners of the CLT panels and designed to be completely
186 prefabricated. The connector is composed of an external case made of metal and an inner
187 element made of hardwood. Such a system permits either to connect a series of wall panels
188 (two or more) or to connect the same panels to the foundations.

189 X-RAD is capable of resisting simultaneously both shear and tension loads thanks to the 3D
190 layout of the fully-threaded screws. The use of a single metal connector increases the level

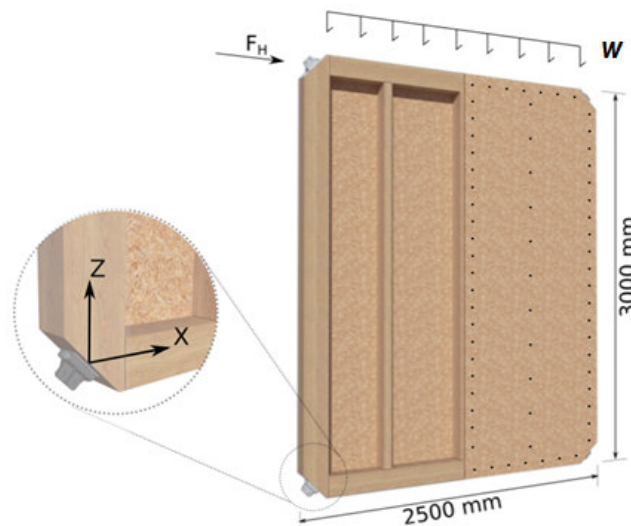
191 of prefabrication and simplifies the calculation and verification processes, allowing a designer
192 controlling the load paths within the structure [19].

193 X-Mini was designed using the knowledge gained while studying the X-RAD connector [20]
194 to be used in single-storey structures. The mechanical behaviour of the steel body of X-RAD
195 was completely re-defined, requiring a new structural characterization for X-Mini.

196 3.3 Geometrical and mechanical properties of the HFT wall system

197 The geometrical properties of the HTF wall system meet the structural requirements of the
198 three housing facilities presented in Section 2 and used as case studies.

199 The inner studs are made of C24 solid wood with section of 60 mm by 100 mm, while the top
200 and the bottom beams and the outer studs are made of 100 mm thick CLT members with a
201 section of 140 mm by 100 mm and 180 mm by 100 mm, respectively. The frame is sheathed
202 on both sides with two 15 mm thick OSB/3 panels, connected to the structural frame with 3
203 mm by 80 mm ring nails with a spacing of 100 mm.



204

205 **Figure 5: The Hybrid Timber-Frame (HTF) wall system and the X-Mini**

206 The design of the HTF wall is performed in accordance with the Eurocodes [21], [22] and it
207 considers the most demanding situations that could occur in Italy (in terms of snow load, wind

load and seismic action, respectively). This was done because the HTF modules should be used all over the Italian country, regardless the location where the emergency occurs. The characteristic value of the snow load is assumed equal to 2.45 kN/m^2 (associated to an altitude of 1000 m on the sea level) while the dead loads of the roof elements and the wall modules are assumed equal to 0.75 kN/m^2 and 0.60 kN/m^2 , respectively. A tributary length of 5 m is used to calculate the uniform distributed vertical load acting on the HTF wall. The seismic loads acting on each wall are determined using elastic response spectrum analyses on the three housing facilities considered as case studies in Figure 4. A peak ground acceleration of $0.60g$ and a q -behaviour factor equal to 1.5 were considered, to ensure an elastic (non-dissipative) behaviour with limited damages to the structure also in case of a strong seismic event. The seismic analyses were carried out using 3D Finite Element numerical models in SAP 2000 [23] according the method proposed in [24,25] for LFT systems and also presented in Section 6.

The mechanical behaviour of a HTF wall subjected to in-plane vertical and lateral loads can be described by taking as reference the traditional LFT systems. The vertical loads due to the gravitational actions is transferred to the foundation system via the inner and outer studs. The in-plane stability and mechanical strength of the wall is ensured by the sheathing panels which are connected to the wood-based frame with ring nails. Differently from a traditional LFT, where hold-down and shear connections are adopted, the rigid rocking and the slippage of the wall panel is prevented by the X-Mini located at the bottom corners of the walls. Hence, each X-Mini is simultaneously subjected to a vertical T_z and horizontal T_x load. An analytical model for the design action on X-Mini is reported in [26].

The resulting maximum vertical load w per unit length due to dead and snow loads is equal to 27 kN/m , while the maximum in-plane horizontal load F_H obtained from the seismic analysis is equal to 25 kN (in the cases analysed, the seismic combination always represents the worst case scenario regarding horizontal load). Based on the previous load values, the horizontal

234 (T_x) and vertical $(T_{z,t})$ components acting on each X-Mini are equal to 12.5 kN and 29 kN,
235 respectively.



236 **Figure 6: The X-Mini connection system**

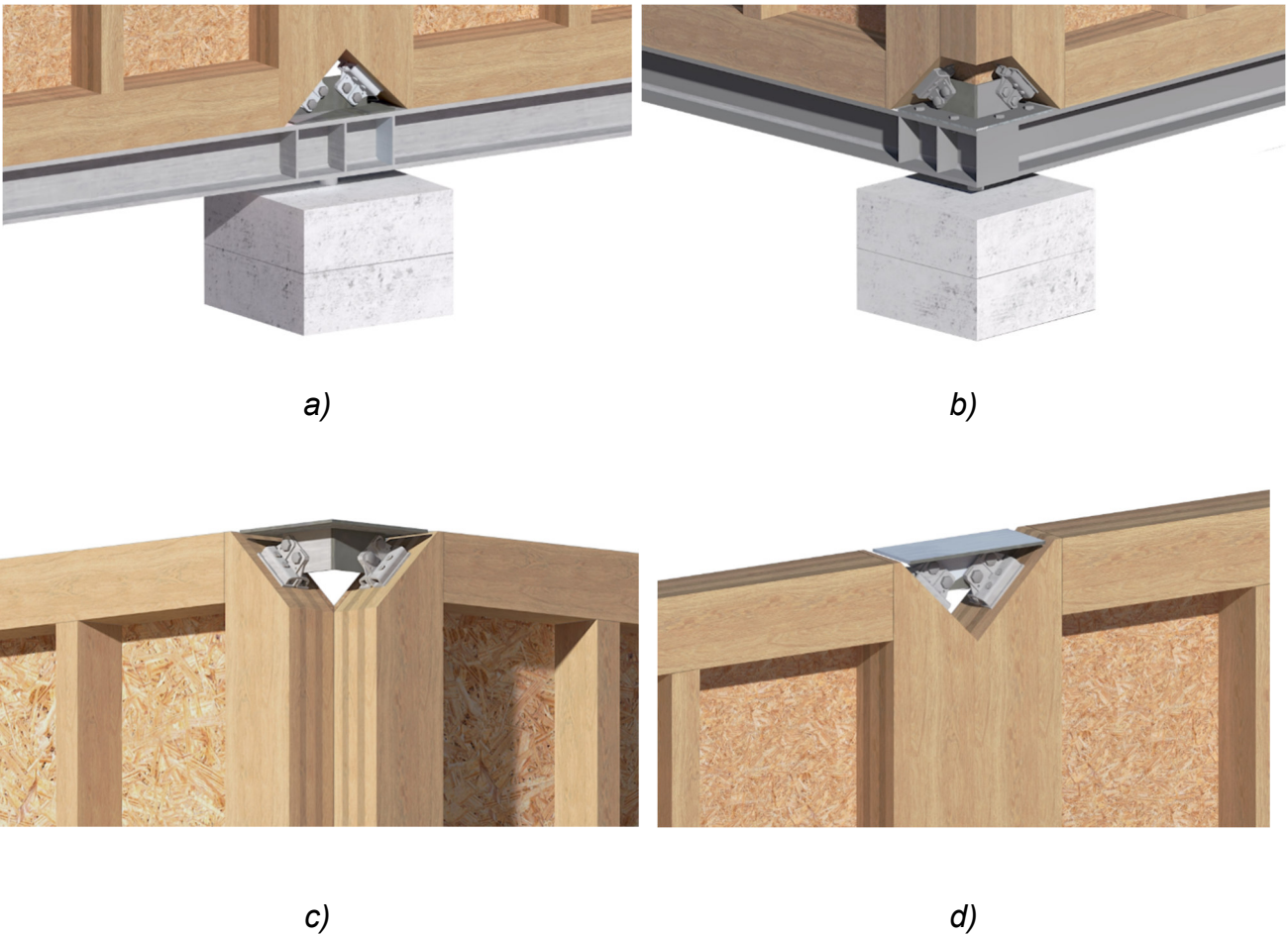
237 **3.4 Foundation system and structural details**

238 The connection of each wall module to the foundations is the most distinctive aspect of the
239 HTF thanks to the use of X-Mini connections as an alternative to traditional anchoring devices
240 (hold-down and angle brackets). Each wall is anchored to the sub-structure system by means
241 of bolted connections between X-Mini and supplementary steel plates which are bolted to the
242 steel beams that compose the foundation grid. Those steel plates are designed to anchor two
243 adjacent modules and, depending on the mutual position of the two HTF walls (either parallel
244 or orthogonal), different typologies have been developed, see Figures 7a and 7b.

245 The grid of steel beams is supported by concrete blocks, which transfer the vertical loads to
246 the ground as a foundation system. Each punctual structural element consists of concrete
247 blocks (60x60x10 cm) connected each other via a cylindrical vertical steel tube equipped with
248 an upper and a lower steel plate. Additional concrete elements could be added depending on
249 the uplift loads due to wind or seismic actions. The whole sub-structure and foundations are
250 designed to meet the requirements of rapid assembly, disassemble and re-use, and do not

251 require any excavation or concrete curing. Differently from the foundations typically used for
252 emergency housing facilities (i.e. concrete platforms), the proposed system is completely
253 removable with a positive impact on the sustainability of the whole constructive process.
254 Moreover, a direct contact of the steel grid base system with the ground is avoided using such
255 punctual foundations, representing an important advantage in terms of durability of the
256 system.

257 Another innovative aspect of the constructive process developed within the TRE3 research
258 project [34] is related to the wall-to-wall joint, see Figures 7c and 7d. Specifically, in traditional
259 LFT systems two adjacent walls are connected using screws; conversely, in the HTF modules
260 those walls are connected by means of a steel plate bolted to two X-Mini located on the upper
261 and lower corners of the wall.



262 **Figure 7: Foundation system and structural details: connection the foundations (a and b) and wall-to-**
263 **wall connection (c and d)**

4. Experimental campaign

An experimental campaign carefully addressed the seismic performance of the HTF system at the connection and at the wall level, respectively. Firstly, monotonic and cyclic tests were performed on the X-Mini connection considering different loading configurations. Monotonic and cyclic full-scale tests were carried out afterwards on the three HTF modules, to analyse in detail their lateral resistance.

4.1 Tests on the X-Mini connection system

Monotonic (M) and cyclic (C) tests were carried out to investigate the mechanical properties of the X-Mini connection system, see Table 1. All the X-Mini used in the tests were connected to 100 mm thick CLT specimens (3-layers 33-34-33 mm) by means of four fully threaded self-tapping screws with a diameter equal to 9 mm. The dimensions of CLT specimens (800mm x 400mm) were specifically chosen to study the behaviour of the X-Mini regardless the edge distances in order to avoid unexpected failure modes of the specimen. However, it is noteworthy to mention that in the shear-walls full-scale tests the X-Mini were screwed to the CLT outer studs of the framed wall, dimensioned as discussed in previous Sections, with a minimum size equal to 180 mm.

Tests considered four loading configurations, obtained by varying the angle between the axis of symmetry of the X-Mini and the direction of the outer boards of CLT specimens: 0°, 90°, +45° and -45° as shown in Figure 8. Furthermore, the experiments analysed how the length of the screws affects the overall performance of the X-Mini, and three different lengths were considered: 200, 240 and 280 mm, respectively.

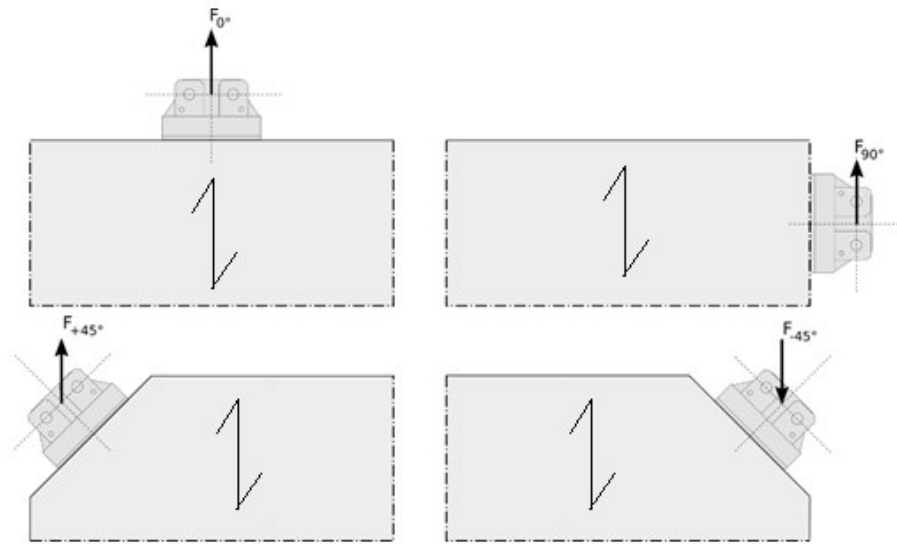


Figure 8: Loading configurations considered in the experimental campaign on the X-Mini

For all four configurations investigated in the tests, the loading direction was set parallel to the outer boards of the CLT specimens. The displacement along the loading direction and the applied load were measured using a LVDT transducer and a 250 kN load cell, respectively. Figure 9 shows the most representative load-displacement curve of each group of tests that was listed in Table 1.

Table 1: Load configurations and screw length for the connection tests

Test	Configuratio n	Screw length [mm]	Loading Protocol
M_0_280_001, M_0_280_002, M_0_280_004 and M_0_280_005	0°	280	Monotonic
M_0_240_006 and M_0_240_007	0°	240	
M_0_200_008 and M_0_200_009	0°	200	
M_90_280_003	90°	280	
M_90_240_010 and M_90_240_011	90°	240	
M_90_200_012 and M_90_200_013	90°	200	
M_+45_240_014 and M_+45_240_015	+45°	240	
M_-45_240_018 and M_-45_240_019	-45°	240	
M_45_280_020 and M_45_240_021	+45°	280	
C_0_280_005	0°	280	Cyclic
C_0_240_001 to C_0_240_004	0°	240	
C_90_240_006 and C_90_240_007	90°	240	

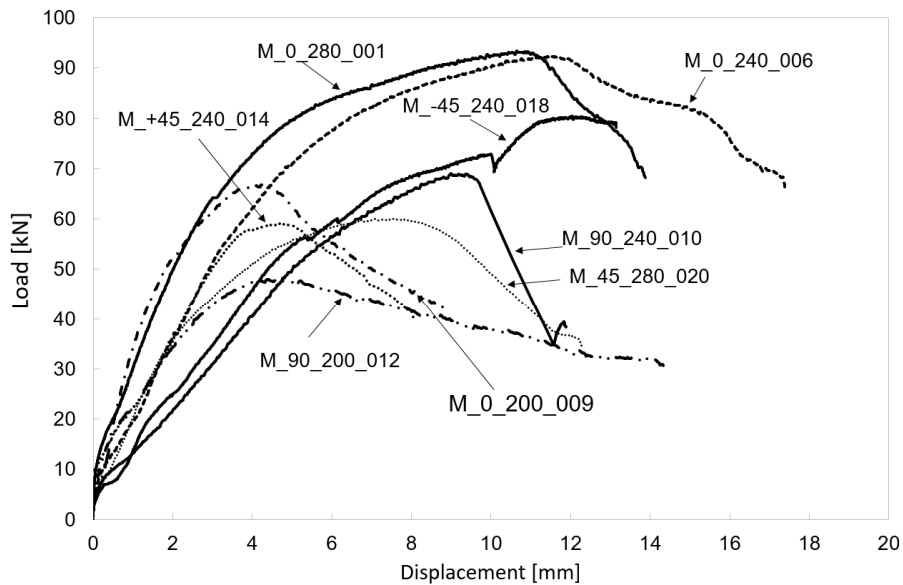


Figure 9: Load-displacement monotonic curves of the X-Mini

From the monotonic tests, the maximum load (F_{max}), the elastic stiffness (K), the displacement at the maximum load (v_{Fmax}) and the failure mode were determined and reported in Table 2 and in Figure 10. Values of the elastic stiffness were determined as the slope of the secant line drawn through the points of the loading curve at 10% and 40% of the maximum load.

The first set of tests (M_0_280_001; M_0_280_002; M_0_280_004; M_0_280_005), carried out by considering screws with a length of 280 mm and an angle of 0° , lead to a maximum load F_{max} between 93.34 kN and 105.57 kN. In all four tests, failure was achieved in the CLT member and was associated to the plug shear failure of the central layer combined with the withdrawal of the screws. Similar values of F_{max} were obtained also when using the screws with a length of 240 mm (M_0_240_006 and M_0_240_007). On the contrary, the two tests carried out using screws with length of 200 mm (M_0_200_008 and M_0_200_009) lead to values of F_{max} equal to 67.72 kN and 66.85 kN, respectively. The specimens assembled using screws of length equal to 200 mm achieved failure due to the withdrawal of the fasteners. Such a mechanism is associated to the shorter threaded length of the screws compared to the results presented above. On the contrary, all screws with length greater than or equal to 240 mm exhibited the failure because of the plug-shear failure of the CLT panel. For this

311 reason, the screws with length of 280 and 240 mm did not show noticeable differences of
312 maximum load.



a)



b)



c)



d)

313 **Figure 10: Failure mechanisms shown in the monotonic tests: a) M_0_240_006, b) M_90_200_012, c)**
314 **M_+45_240_014, d) M_-45_240_018**

315 All tests carried out considering an angle of 90° lead to similar values of F_{max} for screw length
316 equal to 280 mm and 240 mm: M_90_280_003 leads to 67.78 kN, M_90_240_010 leads to
317 69.08 kN and M_90_240_011 leads to 63.57 kN. However, failure was achieved in the CLT
318 panel in test M_90_280_003, while tests M_90_240_010 and M_90_240_011 exhibited the
319 tensile failure of the screws. The experiments carried out considering screws with a length of

200 mm lead to lower values of the maximum load F_{max} (equal to 48.02 kN for M_90_200_012 and 52.37 kN M_90_200_013) than the tests with 240 mm and 280 mm screws.

Tests carried out considering an angle of 45° (M_+45_240_014 and M_+45_240_015) lead to lower values of F_{max} compared to tests performed with an angle of -45° (M_-45_240_018 and M_-45_240_019): such a difference is associated to the loads carried by the X-Mini. In the $+45^\circ$ loading configuration the connection is subjected to a combination of tension and shear, while in the -45° loading configuration the steel plate directly transfers the compressive component of the load to the CLT panel and the X-Mini screws are subjected only to shear.

All cyclic tests were carried out in accordance with the EN 12512 [27] testing protocol and the maximum load $F_{max,c}$, the elastic stiffness K_c , the yield displacement $v_{y,c}$, the yield load $F_{y,c}$, the ultimate displacement $v_{u,c}$ and the ductility μ were determined as described in the same standard. The impairment of strength $\Delta F_{max,1-3}$ between the 1st and the 3rd hysteresis cycles and the corresponding equivalent viscous damping ratios v_{eq} were determined by considering the displacement level where the maximum load $F_{max,c}$ was reached, Figure 11 and Table 3.

The cyclic tests carried out using screws with length equal to 240 mm (tests C_0_240_001 to 004) exhibited values of $F_{max,c}$ between 78.74 kN and 105.58 kN, which were consistent with corresponding maximum loads obtained in the monotonic tests (see tests M_0_240_006 and M_0_240_007). Test C_0_240_001 exhibited the plug shear failure of the central layer of the CLT panel, while test C_0_240_004 achieved the tensile failure of the screws. A similar failure mechanism was also observed in test C_0_280_005, where screws of length 280 mm were used and a maximum load of 94.36 kN was measured. The two cyclic tests carried out with an angle of 90° (C_90_240_006 and C_90_240_007) achieved failure in the CLT panel and showed a maximum load of 65.49 kN and 73.19 kN, respectively, which were consistent with the results of the monotonic tests (F_{max} of M_90_240_010 is equal to 69.08 kN and F_{max} of M_90_240_010 is equal to 63.57 kN).

Table 2: Mechanical properties obtained from the monotonic tests on the X-Mini

Test	F_{max} [kN]	K [kN/mm]	V_{Fmax} [mm]	Failure
M_0_280_001	93.34	22.07	10.6	Panel
M_0_280_002	97.25	26.98	11.6	Panel
M_0_280_004	105.97	19.72	15.1	Screws
M_0_280_005	94.17	24.84	10.8	Panel
M_0_240_006	92.31	15.12	11.5	Panel
M_0_240_007	94.20	16.81	11.5	Panel
M_0_200_008	67.72	57.03	1.7	Panel
M_0_200_009	66.85	30.56	4.2	Panel
M_90_280_003	67.78	30.69	7.4	Panel
M_90_240_010	69.08	8.41	9.0	Screws
M_90_240_011	63.57	6.88	8.3	Screws
M_90_200_012	48.02	24.78	4.4	*
M_90_200_013	52.37	10.39	5.6	*
M_+45_240_014	59.08	12.28	4.6	Panel
M_+45_240_015	66	20.31	5.7	Panel
M_-45_240_018	80.45	11.89	12.0	Panel
M_-45_240_019	89.08	12.38	18.3	Panel
*No failure was observed, test was stopped at a displacement equal to 15 mm				

347 The cyclic tests achieved ductility ratios included between 2.32 and 3.58 when the angle of
348 0° was used, while the test C_90_240_007 exhibited a ductility ratio equal to 1.90.

349 All tests showed strength values significantly higher than the resulting actions obtained from
350 the seismic analysis on the three case studies reported in Section 2 (where the horizontal T_x
351 and vertical $T_{z,t}$ components on each X-Mini were equal to 12.5 kN and 29 kN, respectively).
352 The X-mini connection can hence be considered as a suitable solution for the objectives of
353 the TRE3 research project. However, since only two tests have been performed for each
354 configuration, a higher number of tests will be carried out in future before using the connector
355 in actual structures.

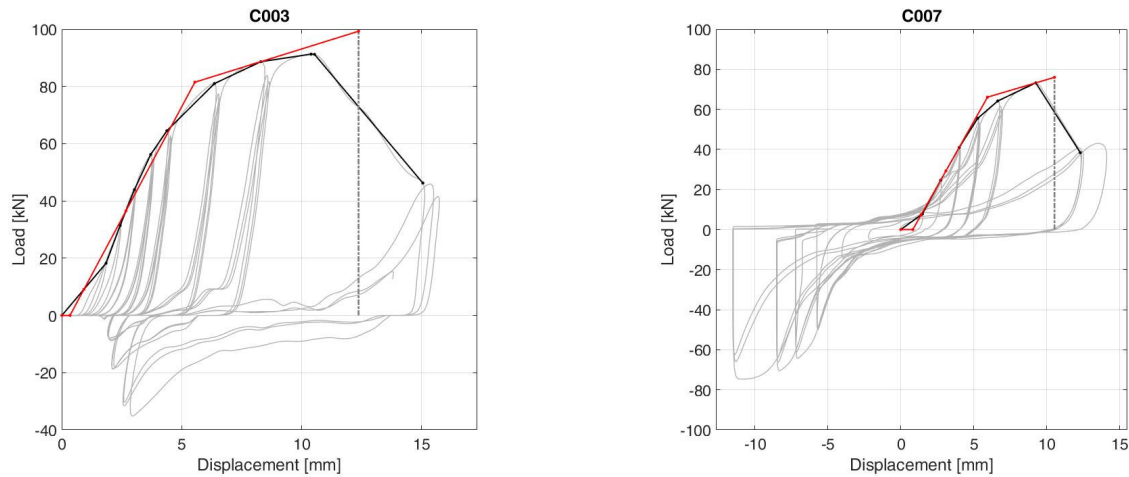


Figure 11: Load-displacement curves for tests C_0_240_003 and C_90_240_007

Table 3: Mechanical properties determined from cyclic tests on X-Mini

Test	$F_{y,c}$ [kN]	$F_{max,c}$ [kN]	$v_{y,c}$ [mm]	$v_{u,c}$ [mm]	K_c [kN/mm]	μ [-]	$\Delta F_{max, 1-3}$ [%]	$V_{eq,1}$ [%]	$V_{eq,3}$ [%]	Failure mode
C_0_240_001	71.54	78.74	4.06	11.11	17.9	2.86	14	6.2	1.9	Panel
C_0_240_002	82.60	93.50	5.88	13.25	15.0	2.34	25	9.0	2.2	Panel
C_0_240_003	81.50	91.30	5.55	12.4	15.6	2.32	12	8.4	2.2	Panel
C_0_240_004	82.68	105.58	5.21	17.85	16.86	3.58	33	13.3	3.4	Screws
C_0_280_005	82.81	94.36	5.48	16.34	15.46	3.04	15	7.9	2.8	Screws
C_90_240_006	-	65.46	-	9.13	7.01	-	10	20	6.7	Panel
C_90_240_007	66.07	73.19	5.94	10.52	12.92	1.90	30	25	14.5	Panel

4.2 Tests on the HTF wall modules

Full-scale tests of the HTF wall modules investigated their lateral resistance in case of a seismic event, see Figure 12. Four specimens with dimensions of 2500 mm x 2500 mm (i.e. two wall-modules, one door-module and one window-module) were tested. The total height of the specimens was reduced from 3000 mm (reported in Section 2) to 2500 mm to allow for a direct comparison with the test results reported in [28] on traditional LFT shear-walls.

To maximise the loads transferred to the X-Mini anchoring devices, no vertical loads were applied on top of the specimens. The inner studs of the framed wall were made of C24 solid

wood while the outer studs as well as the top and bottom beams were made of linear CLT elements. Table 4 lists the geometrical and mechanical properties of the elements used to assemble the HTF walls. In all specimens, OSB/3 sheathing panels with thickness of 15 mm were nailed on both sides of the structural frame with 3x80 mm ring-shank nails and spacing equal to 100 mm and 200 mm along the edge and the centre of the panel, respectively. Furthermore, 9x240 mm fully-threaded screws were used to fasten the X-Mini to the CLT members, with exception of test PT3-WA-02 where 9x280 mm fully-threaded screws were adopted.

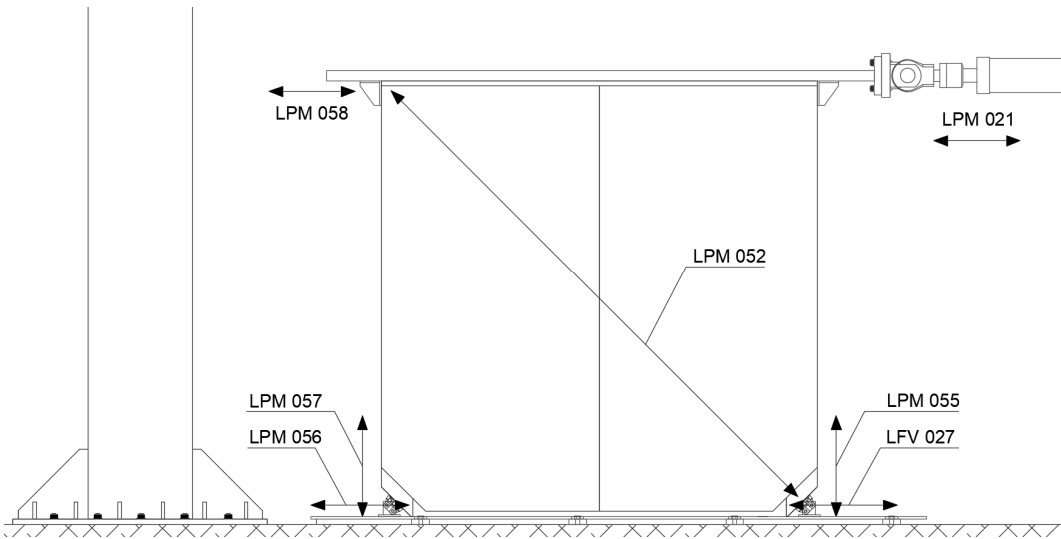


Figure 12: PT3-WI-01 (left) and PT3-WA-02 (right)

Table 4: Wall Test Configurations

Test	Module	Inner studs	Outer Studs	Top/Bottom beams	X-Mini fully-threaded screws
PT3-DO-01	Door	Solid Wood C24; 60mm x 100 mm	CLT 3 layers (33V-34H-33V) 180 mm x 100 mm	CLT– 3 layers (33V-34H-33V) 140 mm x 100 mm	9x240 mm
PT3-WI-01	Window	Solid Wood C24 60mm x 100 mm	CLT 3 layers (33V-34H-33V) 180 mm x 100 mm	CLT– 3 layers (33V-34H-33V) 140 mm x 100 mm	9x240 mm
PT3-WA-01	Wall	Solid Wood C24 60mm x 85 mm	CLT– 5 layers (17V-17H-17V-17H-17V) 180 mm x 85 mm	CLT– 5 layers (17H-17V-17H-17V-17H) 140 mm x 85 mm	9x240 mm
PT3-WA-02	Wall	Solid Wood C24; 60mm x 100 mm	CLT 3 layers (33V-34H-33V) 180 mm x 100 mm	CLT– 3 layers (33V-34H-33V) 140 mm x 100 mm	9x280 mm

377 Six displacement transducers were used to measure the lateral displacement on top of the
 378 wall (LPM 058 and LPM021), the vertical uplift of the bottom corners (LPM 057 and LPM 055)
 379 and the slippage with respect to the ground floor (LPM 056 and LPM027), see Figure 13. In
 380 addition to this, a diagonal wire potentiometer (LPM 052) was installed to measure the shear
 381 deformation of the specimens, while the horizontal load was measured by a 400 kN load cell.



382
 383 **Figure 13: Test set-up and location of measuring devices**

384 The specimens, equipped with two X-Mini connectors, were fixed to the rigid steel foundation
 385 shown in Figure 12 using suitable steel plates of thickness equal to 6mm thick. Each of those
 386 plates was anchored to the foundation using four bolts of diameter equal to 16mm. The cyclic
 387 load was applied to the top face of the HTF using a steel beam as shown in Figure 13; such
 388 an element is equipped with a restraining system that prevents any out-of-plane rotation.

389 The full-scale HTF modules were tested in accordance with the “CNR protocol” described in
 390 [35]. All tests were carried out under displacement control, assuming quasi-static loading
 391 conditions. The cyclic protocol considered in the tests was developed from the rules given in
 392 the EN 12512 [27]. Specifically, the number of cycles after the yielding point given by
 393 EN12512 [27] was increased by introducing a higher number of steps in the hysteresis loop
 394 on the loading curves. All tests assumed a yielding displacement equal to 15mm; this such a
 395 displacement value was deducted from preliminary tests on the HTF system [26] and from

literature results of shear tests on traditional LFT systems [28]. This allowed a direct comparison between the results of the typologies tested.

Results of the wall tests were processed in accordance with the EN 12512 [27] procedure, leading to the assessment of the maximum load F_{max} , the elastic stiffness K , the yield displacement v_y , the yield load F_y , the ultimate displacement v_u and the ductility ratio μ . The impairment of strength $\Delta F_{max,1-3}$ between the 1st and the 3rd hysteresis cycles and the corresponding equivalent viscous damping ratios were calculated at the displacement level where the maximum load F_{max} was achieved, see Table 5 and Figure 14.

Table 5: Mechanical properties determined from cyclic tests on the wall specimens

Test	F_y [kN]	F_{max} [kN]	v_y [mm]	v_u [mm]	K [kN/mm]	μ [-]	$\Delta F_{max,1-3}$ [%]	$V_{eq,1}$ [%]	$V_{eq,3}$ [%]
PT3-DO-01	24.34	30.75	-	-	-	-	-	-	-
PT3-WI-01	37.26	43.06	32.95	77.46	1.10	2.35	13	9.5	8.6
PT3-WA-01	43.03	54.5	15.5	48.59	2.56	3.13	13	14.5	12.1
PT3-WA-02	57.8	66.5	23.01	52.61	2.39	2.29	15	13.3	8.9
Grossi et al. [28] – S_ST_L0	50.7	60.4	19.7	69.7	2.55	3.53	-	-	-

Tests of the two wall-modules exhibited a maximum load equal to 54.5 kN (PT3-WA-01) and 66.5 kN (PT3-WA-02), and an elastic stiffness equal to 2.56 kN/mm (PT3-WA-01) and 2.39 kN/mm(PT3-WA-02), respectively. The values of maximum load and elastic stiffness are similar to those reported in [28] for a traditional LFT wall with 15 mm thick OSB3 panels connected to the timber-frame by means of 2.8/3.1 mm x 60 mm ringed nails with spacing of 100 mm on the edge of the panels and a spacing of 200 mm at the centre of the panel. The traditional LFT system exhibited higher ductility ratio compared to the HTF walls because of the ductile failure mechanism archived in the sheathing-to-framing connections.

As expected, the door-module and the window-module lead to lower values of the maximum loads compared to the wall-module (-43% and -21% of F_{max} compared to test PT3-WA-01).

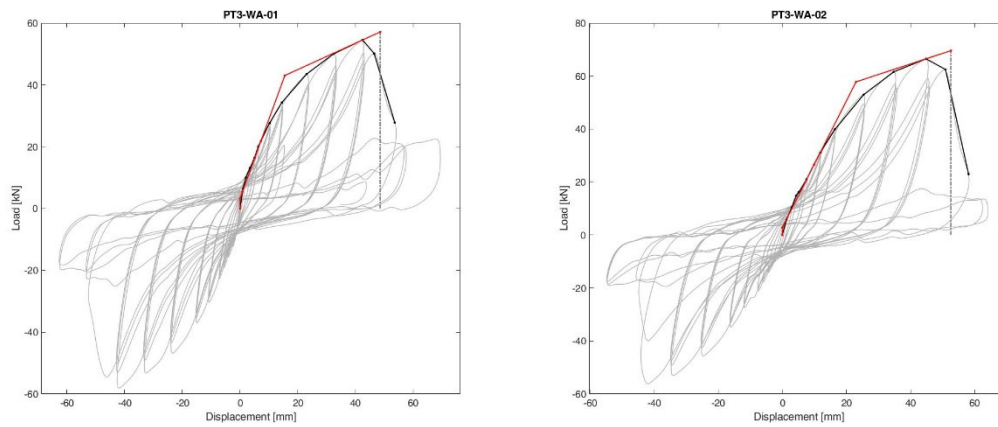


Figure 14: Load-displacement curves of tests PT3-WA-01 (left) and PT3-WA-02 (right)

All four test specimens achieved the failure of the X-Mini connection system, see Figure 15, associated to a combination of plug shear failure of the inner layer of the CLT members and the withdrawal of the screws. The largest value of the ductility ratio was equal to 3.13. Despite the plastic deformations of the sheathing-to-framing nailed connections, no failure of the nails was detected.

The maximum strength of the wall-module with 240 mm screws, equal to 54.5 kN, is consistent with the results obtained from the tests on X-Mini connection with the same length of the screws (240 mm). In fact, tests carried out considering an inclination of 45° exhibited a strength equal to 59.1 kN and 66 kN (M_+45_240_014 and 015, respectively). Due the square shape of the wall (length equal to the height) and the absence of vertical loads, the tensile load due to the rocking of the wall caused a load with inclination approximately equal to 45° with respect to axis of symmetry of the X-Mini.

Further experimental tests will be carried out on the proposed HTF modules to avoid all failure mechanisms in the CLT studs and to improve the performance of the systems.



Figure 15: Failure mechanism observed in tests PT3-WA-01 (left) and PT3-WA-02 (right)

5. Finite element models of the HTF walls subjected to lateral load

A finite element numerical model was developed in SAP2000 [23] to predict the mechanical behaviour of the HFT walls obtained from the full-scale tests.

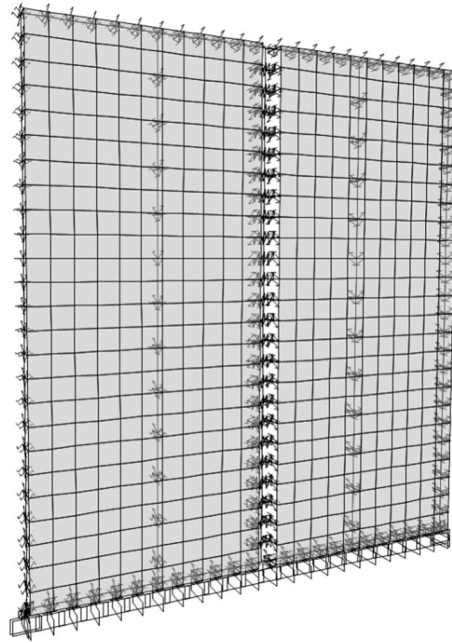
The timber frame and the sheathing panels were modelled through pinned frame elements and shell elements, respectively, see Figure 16. To account for the orthotropic behaviour of CLT, the axial and bending stiffness of the CLT studs and of the top and bottom beams have been defined using the effective elastic modulus E_l according to the theory proposed by Blass and Fellmoser [29], neglecting the elastic modulus in the direction perpendicular to the grain

E_{90} , see Equation 1:

$$E_l = E_0 \cdot \sum_i \frac{t_{l,i}}{t_{tot}} \quad (1)$$

where $t_{l,i}$ is the thickness of the i -th longitudinal layers, t_{tot} is the total thickness of the CLT element and E_0 is the elastic modulus of the solid wood in the direction parallel to the grain, assumed to be equal to 12000 MPa. The in-plane equivalent shear modulus G_{eq} accounts for the torsional and shear deformation of the lamellas and was calculated according to [30,31].

447 In this study, G_{eq} is equal to 582 MPa in the case of a 5-layers CLT panel and is equal to 457
448 MPa in the case of a 3-layers element, respectively.



449

450

Figure 16. Finite element model of PT3-WA-01 in SAP2000

451 The axial and bending stiffness of the solid wood studs are set assuming an elastic modulus
452 E_0 , equal to 11000 MPa. Furthermore, the shear stiffness is defined through the elastic shear
453 modulus $G_{0,mean}$, assumed to be equal to 690 MPa. The sheathing panels are characterized
454 by a plane stress behaviour: the stiffness is defined through the elastic moduli E_v (in vertical
455 direction) and E_h (in horizontal direction) assumed to be equal to 3800 MPa and 3000 MPa
456 depending on the panel orientation, respectively. The shear modulus G_{vh} was assumed to be
457 equal to 1080 MPa.

458 The structural element of the frame (top and bottom beams plus inner and outer studs) are
459 connected to the sheathing panels using nails that are modelled with linear elastic springs (2-
460 joint link element). The nails spacing is equal to 100 mm and the stiffness has been assumed
461 to be equal to 358 N/mm according to [32]. At the base of the wall non-linear gap elements
462 are introduced to simulate the contact of the wall to foundation, characterized by a rigid
463 compression stiffness equal to 10^6 kN/m. The X-Mini have been modelled by means of two

independent multi-linear 1-Joint link elements oriented along the vertical and horizontal directions, respectively. Each link has been characterized by an elasto-plastic behaviour obtained from the load-displacement curves of the experimental tests on the X-Mini, in agreement with the procedure reported in ASTM E2126 [33].

Specimen PT3-WA-01 has been tested connecting the wall to the foundations with two X-Mini connectors, screwed to the CLT frame using screws with a length equal to 240mm. In this case the X-Mini have been modelled assigning to the link elements the load-displacement relationship achieved during test M_+45_240_014. In the same way, test PT3-WA-02 has been modelled assigning to the link elements the bi-linear load-displacement relationship achieved during the test on M_+45_280_020 (where screws with a length equal to 280mm have been used). Finally, the bi-linear load-displacement relationship of test M_-45_240_018 has been assigned to the connector on the compressive side for both tested walls.

Non-linear analyses are performed firstly by applying the self-weight of the wall, followed by an external horizontal load imposed at the top beam. The comparison between experimental and numerical load-displacement relationships (PT3-WA-01 and PT3-WA-02) are reported in Figure 17 and Figure 18.

A good match has been obtained for both models in terms of stiffness, as shown in Figure 17 and Figure 18. The discrepancies of maximum loads are equal to -11% and -16% for the positive and negative quadrant of model PT3-WA-01, respectively. Larger discrepancies in terms of absolute value are obtained for model PT3-WA-01 (equal to -26% and -21% for the positive and negative quadrant respectively), due to the higher strength show by the X-Mini in the wall test than in the connection test.

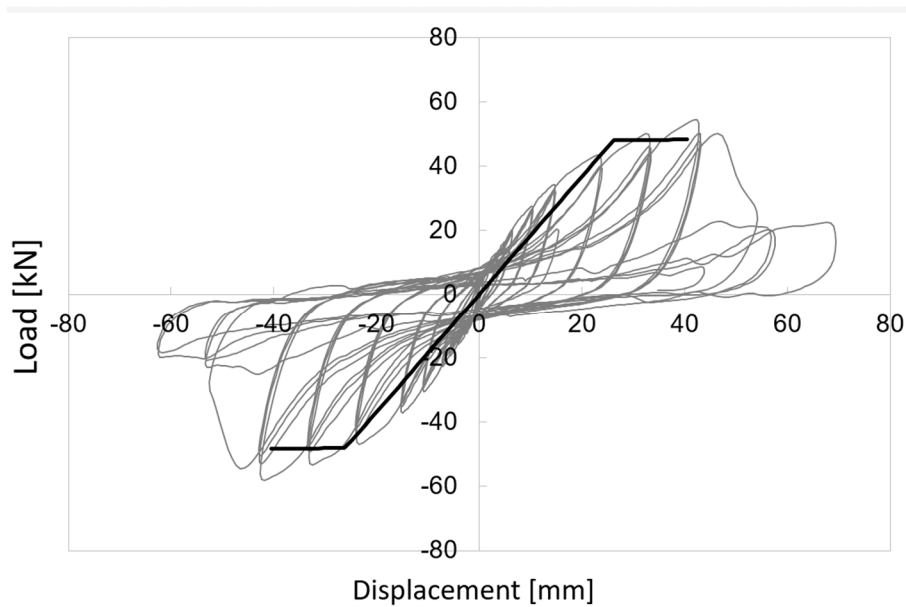


Figure 17. Comparison between experimental behaviour and numerical model of PT3-WA-01

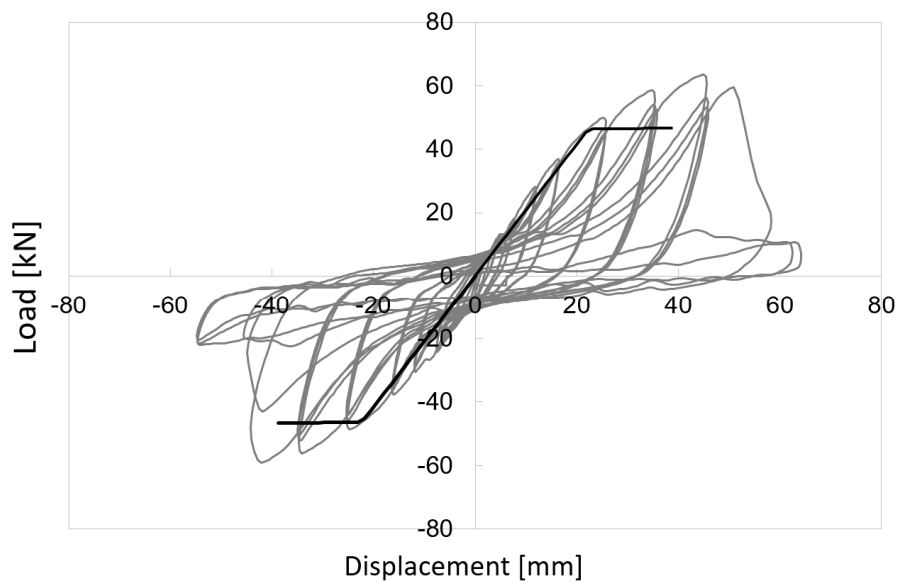


Figure 18. Comparison between experimental behaviour and numerical model of PT3-WA-02

6. Conclusions

This paper presented an innovative constructive system that could be used for emergency housing facilities as an alternative to traditional transitional shelter units. The use of a Hybrid solution for the Timber Frame walls (HTF), obtained from the combination of the traditional LFT system and the more recent CLT system, was allowed by using an innovative connection

497 system called X-Mini. Thus ensured the complete dismantling and re-use of the structural
498 elements and the foundation base systems.

499 The structural performance of the HTF system has been analysed. An extended experimental
500 campaign was carried out to investigate the mechanical behavior of X-Mini by means of
501 monotonic and cyclic testes, showing values of strength significantly higher than those
502 obtained from the seismic analysis of the three housing units used as case studies in this
503 research study.

504 Monotonic tests on X-mini were carried out taking into account two different parameters: the
505 length of screws and four possible directions of the loading force. Cyclic tests have been
506 performed by assuming the external load applied either parallel or perpendicular to the
507 symmetric axis of the connector.

508 Cyclic tests were carried out on four 2500 mm by 2500 mm full-scale HTF walls subjected to
509 lateral loads: two wall-modules, one door-module and one window-module. The maximum
510 strength for the wall-modules was equal to 54.5 kN and 66.5 kN for the wall module with a
511 length of the screw equal to 240 mm and 280 mm respectively. The strength of the wall
512 modules was higher than the value of the lateral seismic action obtained from the seismic
513 analyses on the three housing unit case studies.

514 A finite element model was developed to predict the mechanical behavior of the HTF walls
515 subjected to a lateral load showing a good match with the full scale tests. A good match was
516 obtained for both models in terms of stiffness, whereas a discrepancy between 11% and 26%
517 was shown for the absolute values of maximum loads, due to the higher strength show by the
518 X-Mini in the wall test than in the connection test.

519 Future research will be carried out to achieve a more ductile failure of the X-mini connection,
520 by preventing all failures related to the CLT panels as observed in some of the tests presented

521 in this paper. Further details will be designed and investigated to achieve values of strength
522 suitable also in case of two-storey housing units.

523 **Acknowledgments**

524 The study presented in this paper has been carried out within the framework of the TRE3
525 research project, funded by the Fondazione CARITRO - Cassa di Risparmio di Trento e
526 Rovereto (Trento, Italy). The industrial partners X-Lam Dolomiti (Castel Ivano, Italy) and
527 Rothoblaas (Cortaccia, Italy) are gratefully acknowledged for providing the materials used in
528 the tests. Authors would like to thank Roberto Crocetti (University of Lund, Sweden), Julia
529 Ratajczak and Gabriele Pasetti Monizza (Fraunhofer Italia, Italy) for the valuable suggestions.
530 Mario Pinna and Diego Magnago are gratefully acknowledged for preparation and running the
531 tests. Further acknowledgements are also extended to Andrea Albertini, Daniele Galeaz,
532 Fiammetta Murari and Marica Pidoto. Angelica Pianegonda, Francesca Paoloni and Riccardo
533 Fanti are deeply acknowledged for their precious contribution in the design of the architectural
534 and structural details as well as for the numerical analyses.

536 1. Dipartimento della Protezione Civile (2005), Linee guida per l'individuazione delle aree
537 di ricovero per strutture prefabbricate di protezione civile - Direttiva del Presidente del
538 Consiglio dei Ministri (Gazzetta Ufficiale n. 44 del 23 febbraio 2005). Presidenza del
539 Consiglio dei Ministri - Rome, Italy, *in Italian*.
540
541 2. Dipartimento della Protezione Civile (2005), Manuale tecnico per l'allestimento delle
542 aree di ricovero per strutture prefabbricate di protezione civile - Approvato con Decreto del
543 Capo del Dipartimento della Protezione Civile (n. 1243 del 24 marzo 2005). Presidenza del
544 Consiglio dei Ministri - Dipartimento della Protezione Civile, 2005, Rome, Italy, *in Italian*.
545
546 3. De Berardinis P, De Gregorio S (2014) Temporary systems after the earthquake in
547 L'Aquila. WIT Transactions on The Built Environment 136: 47-58, doi: 10.2495/MAR140041.
548
549 4. Félix D, Branco JM, Feio A, (2013) Temporary housing after disasters: A state of the
550 art survey. Habitat International 40: 136-141, doi: 10.1016/j.habitatint.2013.03.006.
551
552 5. Briani A, Simeone P, Ceccotti A (2012) MAI, IVALSA Modular House. World
553 Conference on Timber Engineering (WCTE) 2012, Auckland, New Zealand.
554
555 6. Filiatrault A, Christovasilis IP, Wanitkorkul A, Van de Lindt JW, (2010) Experimental
556 seismic response of a full-scale light-frame wood building. J Struct Eng 2010;136(3):246–
557 54. [http://dx.doi.org/10.1061/\(ASCE\)ST.1943-541X.0000112](http://dx.doi.org/10.1061/(ASCE)ST.1943-541X.0000112).
558
559 7. Van de Lindt JW, Pei S, Pryor SE, Shimizu H, Isoda H, (2010) Experimental seismic
560 response of a full-scale six-story light-frame wood building. J Struct Eng
561 2010;136(10):1262–72. [http://dx.doi.org/10.1061/\(ASCE\)ST.1943-541X.0000222](http://dx.doi.org/10.1061/(ASCE)ST.1943-541X.0000222).
562
563 8. Seim W, Kramar M, Pazlar T, Vogt T, (2015) Osb and gfb as sheathing materials for
564 timber-framed shear walls: Comparative study of seismic resistance. Journal of Structural
565 Engineering, Volume 142, Issue 4. doi: 10.1061/(ASCE)ST.1943-541X.0001293.
566
567 9. Tomasi R, Sartori T, Casagrande D, Piazza M, (2015) Shaking table testing of a full-
568 scale prefabricated three-story timber-frame building. J Earthquake Eng 2015;19(3):505–
569 34. <http://dx.doi.org/10.1080/13632469.2014.974291>.
570
571 10. Casagrande D, Grossi P, Tomasi R. (2016) Shake table tests on a full-scale timber-
572 frame building with gypsum fibre boards. Eur J Wood Wood Prod 2016;74(3):425–42.
573 <http://dx.doi.org/10.1007/s00107-016-1013-6>.
574
575 11. Izzi M, Casagrande D, Bezzi S, Pasca D, Follesa M, Tomasi R, (2018) Seismic
576 behaviour of Cross-Laminated Timber structures: A state-of-the-art review. Engineering
577 Structures Volume 170, 1 September 2018, Pages 42-52 doi:
578 10.1016/j.engstruct.2018.05.060
579
580 12. Ceccotti A, Sandhaas C, Okabe M, Yasumura M, Minowa C, Kawai N (2013) SOFIE
581 project - 3D shaking table test on a seven-storey full-scale cross-laminated building.
582 Earthquake Engineering & Structural Dynamics, 42(13): 2003-2021, doi: 10.1002/eqe.2309.

- 584 13. Flatscher G, Schickhofer G, (2015) Shaking-table test of a cross-laminated timber
585 structure. Proceedings of the ICE - Structures and Buildings, 168(11): 878-888, doi:
586 10.1680/stbu.13.00086.
587
- 588 14. Popovski M, Gavric I, (2016) Performance of a 2-story CLT house subjected to lateral
589 loads. StructEng 2016; 142(4):E4015006, [http://dx.doi.org/10.1061/\(ASCE\)](http://dx.doi.org/10.1061/(ASCE)ST.1943541X.0001315)
590 ST.1943541X.0001315.
591
- 592 15. Kawai N, Miyake T, Yasumura M, Isoda H, Koshihara M, Nakajima S, Araki
593 Y, Nakagawa T, Sato M, (2016) Full scale shake table tests of five story and three story CLT
594 building structures. In: World Conference on Timber Engineering (WCTE), Vienna, Austria;
595 2016.
596
- 597 16. Yasumura M, Kobayashi K, Okabe M, Miyake T, Matsumoto K. (2016) Full-scale tests
598 and numerical analysis of low-rise CLT structures under lateral loading. J Struct Eng
599 2016;142(4):E4015007. [http://dx.doi.org/10.1061/\(ASCE\)ST.1943-541X.0001348](http://dx.doi.org/10.1061/(ASCE)ST.1943-541X.0001348).
600
- 601 17. ETA-15/0632 (2015) X-RAD: Three-dimensional nailing plate. OIB-Austria, Vienna,
602 Austria.
603
- 604 18. Polastri, A., Brandner, R., Casagrande, D. (2016) Experimental analysis of a new
605 connection system for CLT structures, Structures and Architecture - Proceedings of the 3rd
606 International Conference on Structures and Architecture, ICSA 2016, pp. 119-127. ISBN:
607 978-113802651-3
608
- 609 19. Polastri A, Giongo I, Angeli A, Brandner R, (2018) Mechanical characterization of a
610 pre-fabricated connection system for cross laminated timber structures in seismic regions.
611 Engineering Structures, doi: 10.1016/j.engstruct.2017.12.022.
612
- 613 20. Polastri A, Giongo I, Piazza M, (2017) An innovative connection system for CLT
614 structures. Structural Engineering International, 27 (4), 502-511, doi:
615 10.2749/222137917X14881937844649.
616
- 617 21. EN 1995-1-1:2004/A2 (2014) Eurocode 5: Design of timber structures. Part 1-1:
618 General. Common rules and rules for buildings. CEN, Brussels, Belgium.
619
- 620 22. EN 1998-1:2013, Eurocode 8 (2013) - Design of structures for earthquake resistance
621 part 1: General rules, seismic actions and rules for buildings, (2013). Brussels, Belgium:
622 CEN, European Committee for Standardization.
623
- 624 23. SAP2000 [Computer software]. Computers and Structures America, Berkeley, CA.

- 626 24. Casagrande D, Rossi S, Tomasi R, Mischi G, (2016) A predictive analytical model for
627 the elasto-plastic behaviour of a light-timber-frame-shear-wall, *Constr Build Mater* 2016,
628 102:1113–26, DOI: 10.1016/j.conbuildmat.2015.06.025
629
- 630 25. Casagrande D, Rossi S, Sartori T, Tomasi R, (2012) Analytical and numerical analysis
631 of timber framed shear walls. *World Conference on Timber Engineering 2012, WCTE*
632 2012,5, pp. 497-503.
633
- 634 26. Izzi, M, Casagrande, D, Sinito, E, Pasetto, G, Polastri, A, (2017) Experimental tests on
635 a hybrid timber-frame wall system (2017) *International Journal of Computational Methods*
636 *and Experimental Measurements*, 5 (6), pp. 872-883. www.witpress.com/journals/cmем,
637 doi: 10.2495/CMEM-V5-N6-872-883
638
- 639 27. EN 12512 (2001) Timber structures – Test methods –cyclic testing of joints made with
640 mechanical fasteners. Brussels, Belgium: CEN; 2001.
641
- 642 28. Grossi P, Sartori T, Tomasi R, (2015) Tests on timber frame walls under in-plane
643 forces: Part 2. *Proceedings of the Institution of Civil Engineers: Structures and Buildings*,
644 168 (11), pp. 840-852. doi: 10.1680/stbu.13.00108.
645
- 646 29. Blass H.J, Fellmoser P, (2004) - Design of solid wood panels with cross layers, in
647 *Proceedings of the 8th World Conference on Timber Engineering, Lahti, Finland 2004. Vol.*
648 *2. 2004, WCTE 2004 Secretariat, Helsinki. p. 543-548.*
649
- 650 30. Bogensperger T, Moosbrugger T, Silly G, (2010), *Verification of CLT-Plates under*
651 *loads in plane, The World Conference on Timber Engineering, WCTE, Riva del Garda (Italy).*
652
- 653 31. Brandner R, Dietsch P, Dröscher J, Schulte-Wrede, Kreuzinger H, Sieder M. (2017) -
654 *Cross laminated timber (CLT) diaphragms under shear: test configuration, properties and*
655 *design; Construction and Building Materials*, 147, 2017, pp. 312-327
656
- 657 32. Sartori T, Tomasi R, (2013) Experimental investigation on sheathing-to-framing
658 connections in wood shear walls *Engineering Structures*, 56, pp. 2197-2205.
659 doi: 10.1016/j.engstruct.2013.08.039
660
- 661 33. American Society Standard Method (ASTM) E2126-11 (2018) - Standard Test Methods
662 for Cyclic (Reversed) Load Test for Shear Resistance of Vertical Elements of the Lateral
663 Force Resisting Systems for Buildings.
664

- 665 34. Sinito E, Casagrande D, Izzi M, (2018) The TRE3 research project: a hybrid timber-
666 frame wall system for emergency housing facilities, Proceedings of World Conference
667 of Timber Engineering, WCTE 2018, Seoul, Republic of South Korea
668
- 669 35. Casagrande D, Bezzi S, D'Arenzo, G, Schwendner, S, Polastri, A, Seim, W, Piazza,
670 M, (2020), A methodology to determine the seismic low-cycle fatigue strength of timber
671 connections, Construction and Building Materials, 231, 2020, DOI:
672 10.1016/j.conbuildmat.2019.117026